

Measure of water concentration in atmosphere via photoacoustic effect

Alberto Appoloni, Nicolò Chino

June 24, 2024

Abstract

The goal of this paper is to find the concentration of water in the laboratory via photoacoustic effect. Firstly a test of the apparatus is carried out in order to measure the CO_2 concentration. The result is $n_{CO_2} = 517 \pm 110 \text{ ppm}$ which is compatible with the global average CO_2 concentration: 426.90 ppm . Then, the water concentration is found by injecting air into the photoacoustic cell, employing two filters to select the passing wavelength that excites water molecules: one narrower and the other one wider. The first result shows that $n_{H_2O}^{wider} = (1.9 \pm 0.5)\%$, which is consistent with the measurements from the meteorological station in the laboratory on June 4th in the morning, i.e. $n_{H_2O}^{lab} = (1.8 \pm 0.1)\%$. Additionally, $n_{H_2O}^{narrower} = (2.0 \pm 0.6)\%$ aligns with the meteorological data obtained in the afternoon of the same day: $n_{H_2O}^{lab} = (1.9 \pm 0.1)\%$.

Consequently, Argon and Nitrogen, instead of air, are used to extrapolate the H_2O concentration. This is performed to study the signal variations using a gas similar to air (N_2) and the other one very different (Ar). The results obtained with both gases are compatible with those of the air, although with less accuracy and only if the assumption of non-dry gas is correct.

Finally, a signal stability analysis is carried out to examine the signal response as a function of time, varying some external parameters. It is done to understand what happens inside the cell in terms of condensation and evaporation of water vapour and energy dissipation via collisions of the gas inside the photoacoustic cell. Then, air is demonstrated as the best gas to perform the measure of H_2O concentration in atmosphere not only for its results accuracy, but also for the higher speed at which the signal stability is reached.

Contents

1	Introduction	5
2	Experimental setup and Methods	7
2.1	Carbon Dioxide Calibration	8
2.2	Water Calibration	9
2.3	Signal Stability	10
3	Data analysis and discussion	13
3.1	Calibration	13
3.1.1	Carbon Dioxide	13
3.2	Water	14
3.2.1	Air	14
3.2.2	Argon	16
3.2.3	Nitrogen	18
3.3	Stability analysis	20
3.3.1	Condensation and Losses	21
3.3.2	Argon	22
3.3.3	Nitrogen	24
3.3.4	Air	26
4	Conclusion	31

Chapter 1

Introduction

The photoacoustic effect is a physical phenomenon that can be used to measure the concentration of a gas in a sample. It exploits the interaction between light and gas to generate sound waves, which can be detected and analysed to determine the gas concentration. The sample, which contains the analysing gas, is illuminated via an infrared light beam which is modulated at an acoustic frequency. This light excites the roto-vibrational modes of the gas, which, when de-energized to the ground state, generates a periodic heat gradient, leading to a periodical pressure change, that can be observed as an acoustic signal. The acoustic waves can be analysed via a microphone.

In order to describe mathematically the photoacoustic signal we can exploit the Lambert-Beer law: if we have a beam of infrared power P_0 , P_{tr} : transmitted power, d : absorption path length, σ : absorption cross-section per molecule, n : number of absorbing molecules per cm^3 . The transmitted power can be written as:

$$P_{tr} = P_0 e^{-dn\sigma} \quad (1.1)$$

so the absorbed power: P_{abs} :

$$P_{abs} = P_0 - P_{tr} = P_0(1 - e^{-dn\sigma}) \simeq P_0 dN\sigma \quad (1.2)$$

The last equivalence is valid in the limit of a small exponential argument namely when the concentration N of the gas that we want to analyse is typically less than a few per cent. So the photoacoustic effect can provide a way to determine the concentration of the species interacting with infrared light.

Lastly, we have to mention the tool to capture the desired signal into a noise sea: the lock-in amplifier; indeed the acoustic signal generated by the relaxation of the roto-vibrational modes of the studied gas species can be quite small compared to other noise sources. The lock-in amplifier works by multiplying the microphone signal by a reference-modulating signal allowing an improvement of the signal-to-noise ratio. The result of the multiplication produces 2 components: one at a zero frequency(DC component) and one at double the frequency compared to the reference frequency. The signal is then filtered via a low-pass filter to maintain just the DC component which is proportional to the amplitude of the original signal of interest. The frequency of the reference is chosen at the resonant frequency of the photoacoustic cell to maximise the signal compared to

the noise.

In this relation, firstly, we find CO_2 and H_2O concentrations in the lab by exploiting a calibration curve using air. Then, we try to find the calibration curve of H_2O using, instead of air, argon and nitrogen.

Chapter 2

Experimental setup and Methods

The experimental setup is composed of a power supplier which is used to heat the filament, we set as value of current: $I_{fil} = (8.70 \pm 0.02)A$ and voltage: $V_{fil} = (5.91 \pm 0.01)V$ so the power supplied to the filament will be: $P_{fil} = IV = (51.02 \pm 0.02)W$, we controlled that the values of current and voltage remain constant for all the time of the experience.

After the filament, there is a chopper used to modulate the light beam which is set at the resonant frequency of the photoacoustic cell for each gas studied: $f_{air} = (822 \pm 2)Hz$, $f_{Ar} = (762 \pm 2)Hz$, $f_{N_2} = (839 \pm 2)Hz$, the value is slightly tuned to match the signal maximum when we vary CO_2 or H_2O concentration. Then, the beam is collimated thanks to the collimator tube. Subsequently, the beam passes through an infrared filter to select the correct wavelength in order to excite the modes of the gas we want to analyse. One optical filter is used for CO_2 while two filters are available for H_2O : the narrower allows the transmission of light in the bandwidth ranging from $6.4\mu m$ to $6.8\mu m$, while the wider in the bandwidth in the $5.6\mu m$ to $6.8\mu m$ with difference transmittance that are reported below:

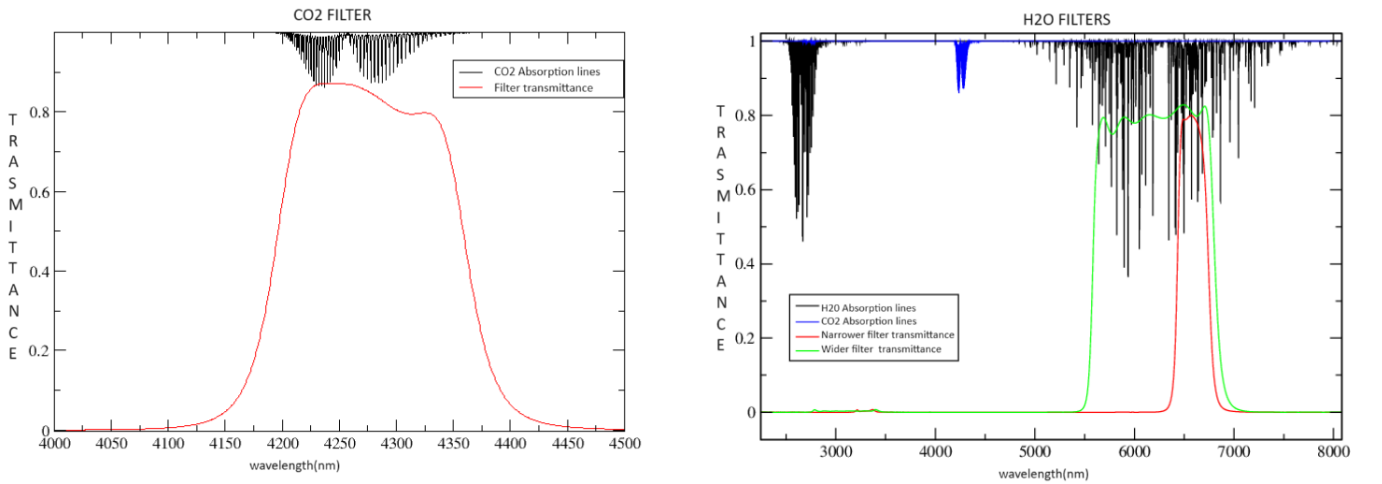


Figure 2.1: Transmittance for CO_2 and H_2O Filters

So the beam enters into the photoacoustic cell in which in the "entrance 1" is located the pressure gauge used to measure the pressure inside the chamber, while in the "entrance 2" the gas is let in. A microphone is connected to the chamber to detect the signal, it is linked firstly to a preamplifier which is linked to a lock-in amplifier. A membrane pump is connected to the photoacoustic cell to empty the chamber after each measurement, it allows us to reach a pressure of $P_{cell}^{min} = (1 \pm 0.2)mbar$.

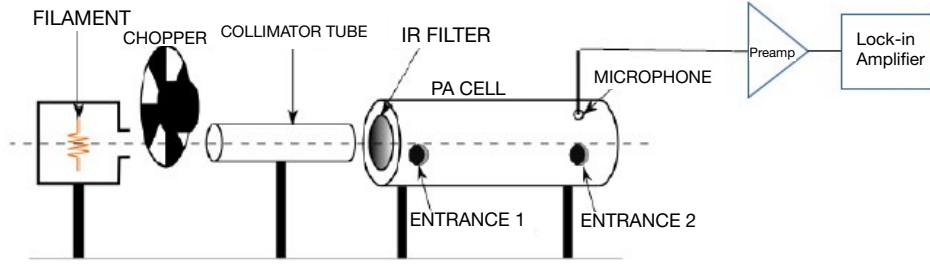


Figure 2.2: Schematic image of our experimental set-up of the photoacoustic part

Then for the first part of the experiment, we focus on doing a calibration curve to obtain the more accurate data on the presence of firstly CO_2 and secondly H_2O , in the atmosphere. In the second part, we try to find an explanation more detailed on the process inside the photoacoustic cell, moving the focus to the stability of the tension value obtained from the lock-in amplifier during a long time exposition: about 10 – 15 minutes. We register every value every 15 seconds changing the injected gas (air, Ar and N_2), the pressure of that gas (only for N_2) and how we let in the gas inside the photoacoustic cell: very fast reaching $(840 \pm 1)mbar$ (we can't be very infinitely precise at which pressure stop the entrance of gases and because of the oscillation at the very beginning are more pronounced, since the system has to find its momentary equilibrium) in about 30 seconds, or very slow: reaching $(840 \pm 1)mbar$ in approximately 15 – 20 minutes letting into the cell $2mbar$ of the gas per time.

2.1 Carbon Dioxide Calibration

For the CO_2 calibration, we make a dynamic measurement by means of two flow meters: at each measurement, a constant value of air flux is let in, while the CO_2 flux is varied in such a way to change the concentration of CO_2 inside the chamber. To perform a single measurement it takes ten minutes with the pump running to mix enough the gases, then the chamber is closed, and it takes another five minutes of measuring the signal for the signal to stabilize.

2.2 Water Calibration

For the H_2O calibration, we make a static measurement: the chamber is first emptied using the membrane pump, then pure water vapour is let in until the correct pressure is reached and finally the other gas enters until approximately 840mbar is reached. The maximum water vapour pressure that we can set is $P_{H_2O}^{max} = (28.0 \pm 0.5)\text{mbar}$ and we take the other points decreasing this value of 2mbar . To select precisely the correct pressure two pinhead valves are used: one for the water vapour pressure and one for the other gas pressure. The concentration of water vapour will be, then, the ratio between the water vapour pressure and the total final pressure. From the outset, it was recognized that condensation in the photoacoustic cell might result in a loss of time in obtaining a correct value of voltage from the lock-in amplifier. Consequently, the initial measurement is conducted within the cell at the maximum water pressure that could be generated in a relatively brief period. This measure represents the most unfavourable condition for condensation and then set a maximum of time waiting to take the measure. Subsequently, the values of the lock-in and pressure are recorded in order to ascertain the point at which all the condensed water would have re-gasified within the cell. The graph of this measure is reported in 3.5 from which we estimate that 11 minutes are enough to proceed to take the measure. Moreover, during the registration of the values, we ascertain whether there is a visible presence of condensation. We observe that approximately 250 seconds elapse (with air) before the condensation dissipates entirely. This is the point at which the slope of the linear increase in pressure within the cell undergoes a change. Prior to this point, we estimate a de-gasification process, which is evidenced by the observation of losses. These losses are smaller in magnitude than those observed during the preceding 250 seconds but a deeper analysis will be done in the next chapter.

To create pure water vapour we have to boil water at room temperature, which is the temperature at which we want to do our measurements, since our aim is to measure the water concentration in the atmosphere and then at the temperature of ambient. In order to do so we decrease the pressure inside a glass chamber containing water using a rotary pump. This water container is connected to another glass container which must be filled only with water vapour and in order to obtain it, the rotary pump must create a vacuum in both containers: to boil the water in one container and to empty the other. A metallic plate to put between the chopper and the collimator tube is also used to estimate the background noise. This noise will be subtracted from the signal for each measurement which are produced in good approximation by the chopper that moves the air at a frequency that it is perfectly at the resonance one and that can be removed only by doing a vacuum around all of the setups. Furthermore, it should be noted that this method of modifying the air produced by the chopper, which is situated behind a wall and not a cylindrical empty tube, can cause variation in the air based on fluid dynamics. For instance, the air that is propagated towards the light source may bounce back and increase the estimation of noise. However, it can be assumed that the change in noise can be neglected in the first approximation. Moreover, the measurement of the noise produced by the chopper is a challenging task for another reason, both in terms of quantification and measurement. Indeed we observe that the noise values vary depending on the distance at which the chopper is positioned relative to the beam collimator, as well as the depth at which it is inserted. Therefore, each measurement is subject to a certain degree of statistical variation, even if we fix a

specific point to ensure at least a consistency across all measurements. However, this approach does not allow for a precise measurement.

To have different ideas on the results that we can obtain using a gas that does not contain H_2O ; we use, as we said previously, not only air but also Ar and N_2 . In this case, the filter is not changed. Following the initial measurements with air, it is sufficient to utilise a narrower filter in order to achieve greater precision in identifying which atom is to be excited. This should be limited to the H_2O atoms.

2.3 Signal Stability

As we saw from the graph of the signal during the long-time exposition of water pressure $P_{H_2O} = (28 \pm 0.5) mbar$ inside the cell with air 3.5: an initial increase in the voltage value is observed, followed by a stabilization phase with a minimal tendency towards a decline. This stabilization phase commenced when condensation ceased to be visible. Furthermore, measurements are conducted at varying levels of humidity, with the most common values being $P_{H_2O}^{high} = (22.0 \pm 0.5) mbar$ and $P_{H_2O}^{low} = (6.0 \pm 0.5) mbar$. However, these are occasionally adjusted by a few $mbar$ to accommodate specific experimental requirements. Initially, the objective is to ascertain whether the observed qualitative behaviour was consistent across a range of humidity levels, both high and low. This is followed by the establishment of the two distinct reported values of H_2O pressure values, as benchmark for subsequent consideration at different humidity level: "high" and "low".

Also in this second part of the experiment we use different gases that are identical to those used in the calibration phase of the experiment, namely Ar and N_2 . The change in the gas that we introduce in the photo-acoustic cell with H_2O is done because we want to understand in which way the different gases with which H_2O interact, can enhance or inhibit the non-radiative relaxing process of H_2O atoms, and if this change could vary also the qualitative trend of the signal.

Finally, with N_2 , we vary also the injected gas pressure using $P_{N_2}^{low} = (2.0 \pm 0.2) bar$ and $P_{N_2}^{high} = (6.0 \pm 0.2) bar$. Then, with air and N_2 , we compare also 2 different ways of letting in the gas inside the photo-acoustic cell as stated in the previous section: this is done to understand if the qualitative behaviour that we measure is something based on the physical meaning of the effect inside the photo-acoustic cell, or caused only by the experimental way of proceeding.

We specify that during all this part of the experiment we will not change the filter because we note that changing it, does not provide much insight into the underlying physics, apart from the differing values of tension observed in the lock-in. Then, as for the previous part when we change the gases, we limit our analysis to the narrower filter

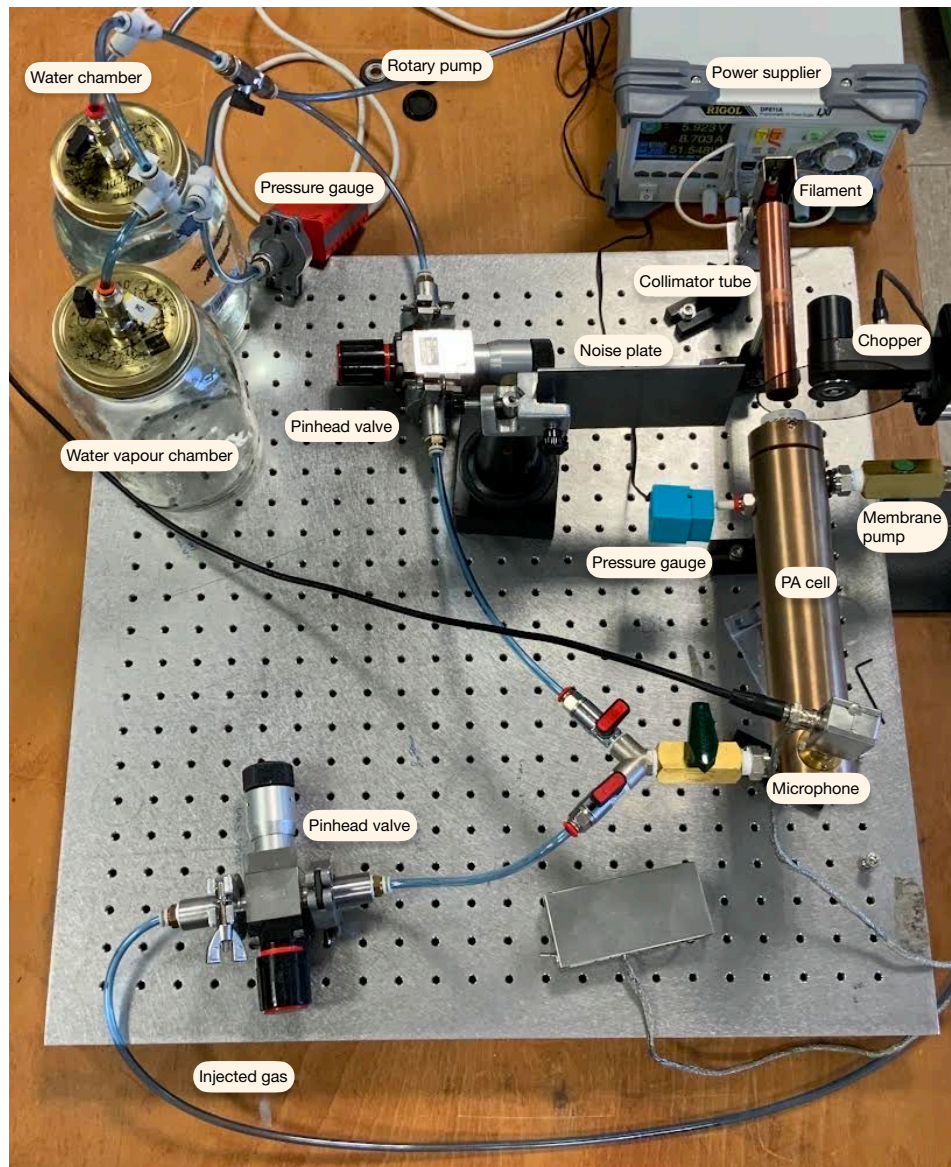


Figure 2.3: Experimental Setup

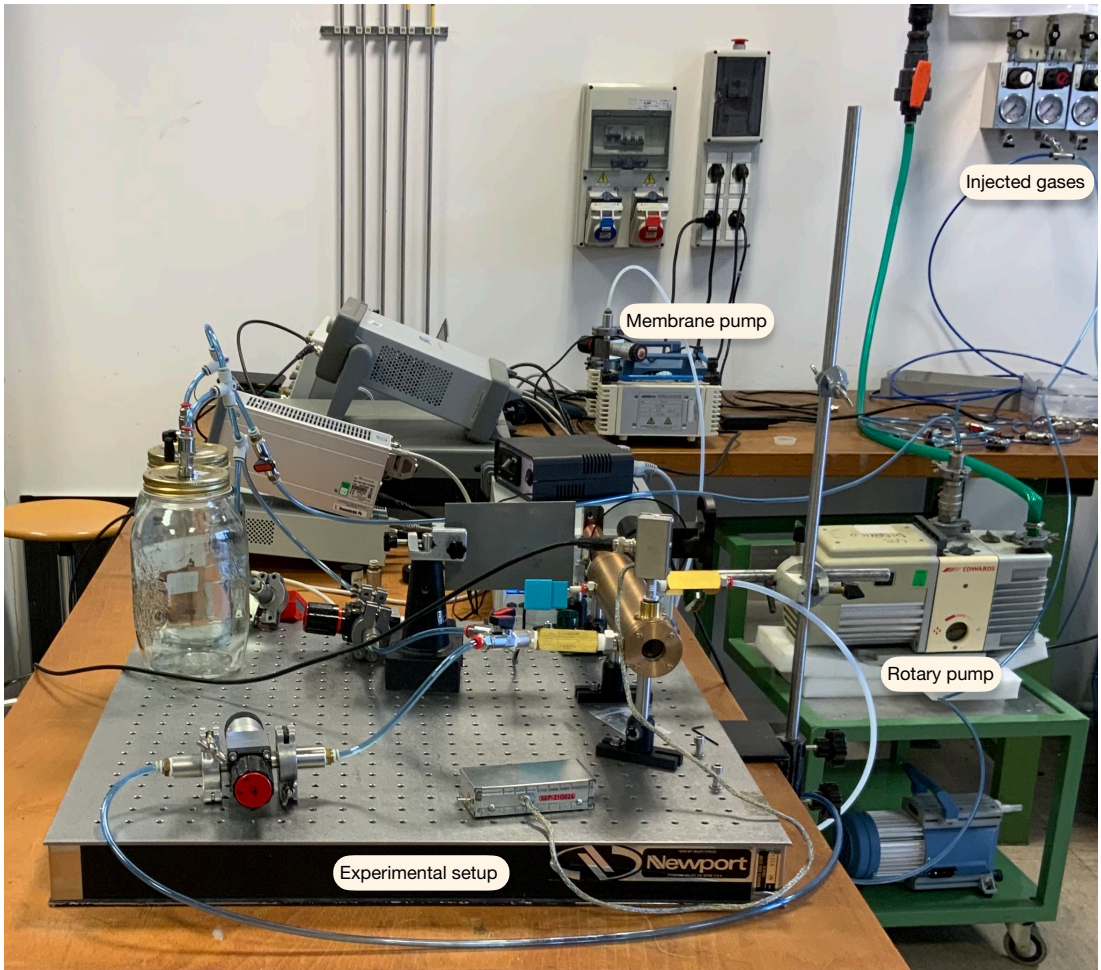


Figure 2.4: Pumps used



Figure 2.5: Meteorological station

Chapter 3

Data analysis and discussion

As we highlighted in the previous section the experiment is subdivided into 2 macro aims: the first one is effectively the measure of the percentage of H_2O inside the atmosphere through a calibration curve, and the second one (which is conducted almost in parallel with the first one) is based on the will to understand which is the main causes of the creation of pressure waves inside the photo-acoustic cell. The calibration is firstly done for CO_2 in the air with a dynamical measurement, and then we move towards the H_2O . Both parts of the experiment with the "main character" the H_2O are done with air, Ar and N_2 . Firstly we discuss the calibration part, secondly, we will discuss the behaviour along time of the signal, even if the second one is quite necessary for the first one, but in this way, it gives more clarity to the paper.

3.1 Calibration

3.1.1 Carbon Dioxide

We saw in the first chapter that the absorbed power, for the case of $n \ll 1$, is equal to:

$$P_{abs} = P_0 d\sigma n \quad (3.1)$$

so the signal that is seen in the lock-in amplifier will be proportional to:

$$V_{li} \propto d\sigma n_{air} + d\sigma n_{CO_2} \quad (3.2)$$

where V_{li} is the lock-in signal and n_{air} is the unknown carbon dioxide concentration. This equation can be fitted via a line:

$$y = mx + q \quad (3.3)$$

where y is the lock-in amplifier signal, $x = n_{CO_2}$, $m = d\sigma$ and $q = n_{air}d\sigma$ so $n_{air} = \frac{q}{m}$.

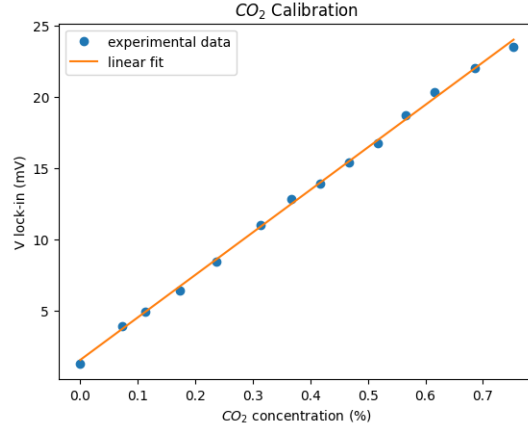


Figure 3.1: Calibration curve for CO_2 concentration in atmospheric air

The results of the fit are $q = 1.6 \pm 0.5 mV$, $m = 29.8 \pm 1.4 \frac{mV}{100}$, so $n_{CO_2} = \frac{q}{m} = 517 \pm 110 ppm$. It can be observed that the error in the measurement is considerable. However, this peculiarity will persist throughout the entirety of the experimental results. Therefore, it is necessary to justify this and to consider it for all future experiments, as it is related to the manner in which the measurements are conducted (and for the physics that we investigate), and will therefore be repeated throughout the entirety of the experiment. The reasons for this significant discrepancy are manifold. The filament that generates photons in the microwave is uncovered, and even minor wind waves from the outside or excessive movement of people around the experimental setup can create non-negligible oscillations. Furthermore, we are performing a linear approximation on an exponential law, which means that our measurements are not in a perfect straight line. Moreover, it is important to consider that, in the case of H_2O , the membrane pump is unable to maintain a residual pressure of less than $1 mbar$ in the photoacoustic cell. Additionally, as will be demonstrated in the second section of the data analysis, there are greater losses in the photoacoustic cell when attempting to maintain a lower pressure inside. Consequently, the uncertainty on the concentration value is likely to be significant.

However, the value is consistent with the current global average CO_2 concentration which is $426.90 ppm$ also because in the laboratory with the door closed there were five people and an additional source of CO_2 : yeast fermentation of the other group, so the global average value could be underestimated for the lab environment.

3.2 Water

3.2.1 Air

The calibration for the water case using air as "background gas" is analogous to the carbon dioxide case:

$$V_{li} \propto d\sigma n_{air} + d\sigma n_{H_2O} \quad (3.4)$$

Two filters are used to make the calibration: one wider and the other one narrower 2.1.

The results of the calibration have to be compared with the concentration value obtained by the meteorology

station in the lab on the calibration day. On the morning of 4th June, there were $T_{room} = (24 \pm 1)^\circ C$, relative humidity: $R_H = (58 \pm 1)\%$, environment pressure: $P_{room} = (978 \pm 2)mbar$. The saturation pressure can be calculated via the semi-empirical Magnus-Tetens formula:

$$P_{sat} = 6.112e^{\frac{17.67T}{T+243.5}} \quad (3.5)$$

that is the maximum pressure of water at a certain T in atmospheric conditions; then the vapour pressure is: $P_{vap} = \frac{R_H P_{sat}}{100}$ that is the effective pressure of H_2O inside air, the "air" pressure (we intend the pressure of air without the contribution of H_2O): $P_{air} = P_{room} - P_{vap}$ and finally the H_2O concentration: $n_{H_2O}^{lab} = \frac{P_{vap}}{P_{air}}$. Then it is conducted a calibration curve with the two filters 2.1 and the obtained graphs are reported below:

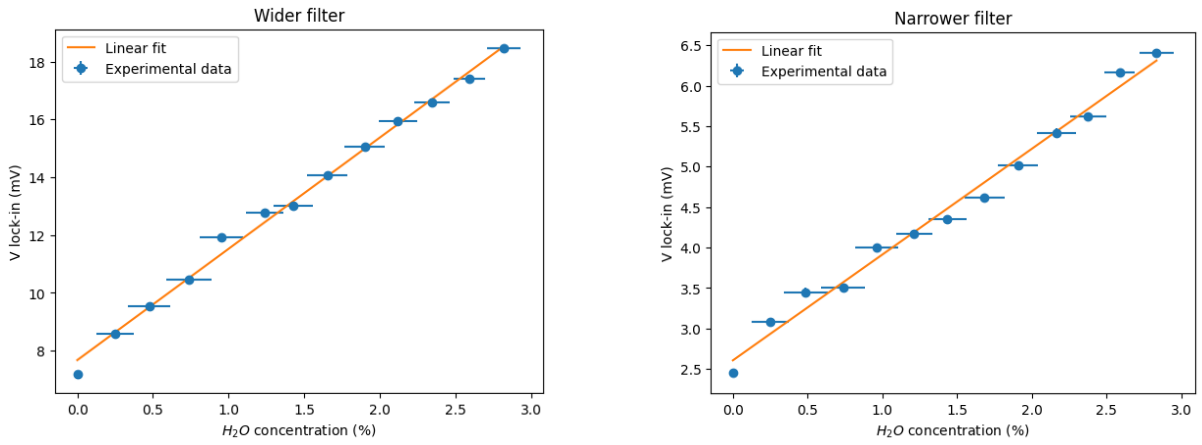


Figure 3.2: Comparison between calibration curves of H_2O with air with the wider filter on the left, and with the narrower on the right

Is easily noted that the error in the measure of voltage from the lock-in is imperceptible. Indeed, as we have already mentioned in the previous chapter, we wait 11 minutes before taking the measurements in order to register a measure that could be as stable as possible. Then the error, since it is estimated based on the still present fluctuations of the value in voltage, is very low that results in a standard deviation of $\sigma_V^{wider} = 0.1mV$ for the wider filter, while $\sigma_V^{narrower} = 0.05mV$ for the narrower one. On the contrary, the error in the concentration is very high indeed, thanks to the stability study 3.5, we have a non-negligible error on the quantity that we insert inside the cell. Leaving the details to that part, now we want only to state that the error on the H_2O that we insert will be quite flat and equal to $\sigma_{P_{H_2O}} = 0.5mbar$ that, as can be noted, create a much more pronounced error on the value at low H_2O concentration rather than to high ones. We highlight moreover that the error in the point at 0 concentration of added water is different because in that case we have not to add any quantity of H_2O and then the only present error is due to the uncertainties of pressure gauges that are very low and can't be seen from the graphs. This clarification will be valid for all the measurements that will be done during all the experiments but are of absolute importance mainly in the calibration part.

We can observe a good agreement with a linear behaviour with both filters having all the points with their error compatible with the linear fit, but we see fewer oscillations from the wider one 3.2(a).

The value obtained exploiting the fit is $n_{H_2O}^{wider} = (1.9 \pm 0.5)\%$ for the wider filter, while with the narrower we obtain $n_{H_2O}^{narrower} = (2.0 \pm 0.6)\%$ which are consistent between themselves and are also consistent with the values given by the meteorological station: $n_{H_2O}^{lab} = (1.8 \pm 0.1)\%$ on 4th June in the morning (when we take the measurements with the wider filter) and $n_{H_2O}^{lab} = (1.9 \pm 0.1)\%$ on 4th of June in the afternoon (when we record the measurements for the narrower filter), noting that this value does not change a lot during the entirety of the day. We report also the angular coefficient of the narrower linear fit. Indeed it is the product $d\sigma$ that constitutes the absorption properties of the background gas. It is something that will become useful in the comparison between different gases: $m_{air}^{narrower} = (1.2 \pm 0.2) \frac{mV}{100}$. The main difference between the two graphs is the smaller signal of the narrower one, as we can expect by the lower transmittance of this one, and because a smaller range of wavelengths is let in the photoacoustic cell.

As we said previously, now we change the gas in which we push H_2O for the calibration using Ar firstly and N_2 secondly without making any comparison between the 2 filters, using only the narrower one as already explained why.

3.2.2 Argon

Changing the gas we have to change the resonance frequency that is found experimentally through the progressive change of the rotation frequency of the chopper until the maximum value of the signal is reached, then we have:

$$f_{Ar}^{res} = (762 \pm 2)Hz.$$

The calibration curve with Ar is reported below:

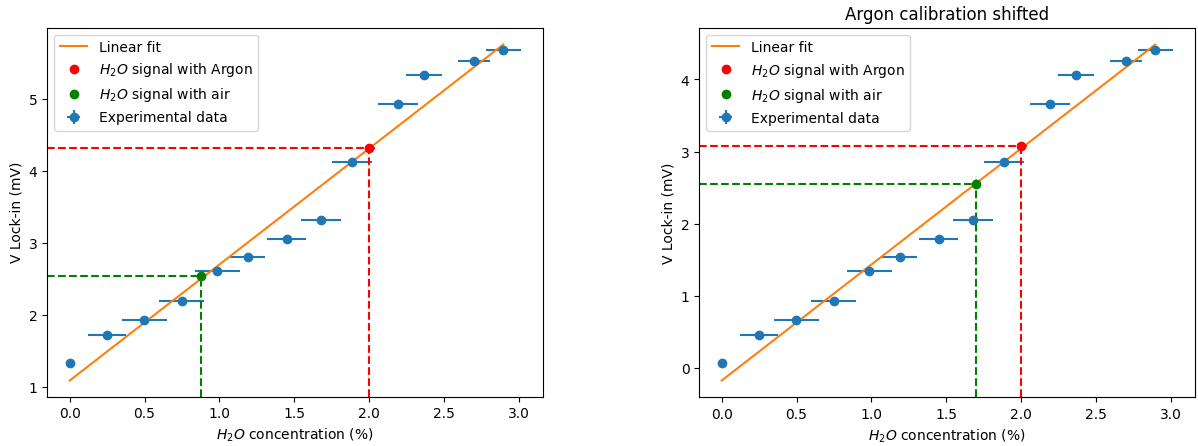


Figure 3.3: Calibration curve using Ar : on the left the value with an offset due to residual humidity, on the right the same plot translated down by $V_{Ar}^{0-conc} = (1.27 \pm 0.05)mV$

in which we highlight to the lecturer, as already did during all the paper, that on the x-axis there is the concentration of H_2O that we push inside the photo-acoustic cell, not the total concentration that there is inside of it. It should be noted that this concentration is the same only in the case of pure dry gases (an assumption that we take for Ar and N_2). Therefore, in order to make a comparison with the calibration with air, it is important to be aware of this fact.

The main difference between using air and some dry gases, i.e. without any presence of H_2O , is that in this case the concentration of H_2O in the atmosphere is taken not as the ratio between the intercept and the slope of the linear regression, because inside the gas we have no H_2O intrinsically and then the signal from the lock-in becomes:

$$V_{li} \propto d\sigma n_{H_2O} \quad (3.6)$$

So, the curve that we plot thanks to the measurements is needed to obtain the measure of the water concentration in air indirectly when, at the end of the registration of values with the known concentration of H_2O , we let in the photo-acoustic cell only air. Then we register that lock-in value and using the linear regression, we trace to the H_2O concentration value. This is the meaning of the green dotted line in the graph 3.3 (the green point is the tension value from the lock-in when we have only the air inside the photo-acoustic cell). So we obtain a water concentration that is: $n_{H_2O}^{Ar} = (0.9 \pm 0.8)\%$ that has to be compared with the value extrapolated from the meteorological station that, in the morning of the 5th of June, is: $n_{H_2O}^{lab} = (2.0 \pm 0.1)\%$ that are completely inconsistent. While, the angular coefficient is: $m_{Ar} = (1.6 \pm 0.4) \frac{mV}{100}$ that is compatible in the uncertainties to what we obtained with water but is higher in a non-negligible way. This is a sign of a different interaction between molecules inside the photo-acoustic cell.

In the plot 3.3 we report with the red point also the value that the lock-in should have recorded if the correct H_2O concentration is detected within the photo-acoustic cell.

We note that this calibration is very "forced" in the sense that the points around the linear regression oscillate a lot, and this is a sign of the fact that probably we need to wait more time to have a more stable measure but this is something that we treat in the second part of the data analysis.

Another peculiar thing is that the values of the tension from the lock-in are higher in absolute value compared to what we obtained with the H_2O calibration using air 3.2 (taking care of doing the comparison between the right measurements of concentrations, as we said at the start of the section). This effect can find a solution from the fact that the thermal conduction of Ar is less than what we have in air and then this causes a more concentrated heating of the molecules inside the cell. This has the consequence of creating a more net temperature gradient, which in turn increases the intensity of the pressure waves. Furthermore, the density of argon gas is greater than that of air due to the difference in mass of the "air molecules", which weigh approximately $29u.m.a.$ (assuming air is 80% nitrogen and 20% oxygen). In contrast, Argon gas has a higher mass, with a value of approximately $39.9u.m.a.$ This leads to more efficient propagation of sound waves within the cell, as it limits the rapid dispersion of heat throughout the gas.

Finally, we note the last thing: at $n_{H_2O}^{Ar} = (0.0 \pm 0.2)\%$ (error given only by the fact that there are losses and we can't evacuate the photo-acoustic cell up to have $P = 0mbar$) we expect to observe a signal in the lock-in that is around $0mV$ because inside the photo-acoustic cell, in this condition, has to be no water. Nevertheless, we register a signal $V_{Ar}^{0-conc} = (1.27 \pm 0.05)mV$. This indicates that there is a process affecting the signal, potentially due to the fact that the Ar gas is not completely dry. It is therefore possible that the signal is caused by the presence of water within the gas. Moreover, we note a particularity: the discrepancy between the voltage observed when the photo-acoustic cell is filled with air (indicated by the green point on the calibration

graph) and the voltage required to achieve a concentration consistent with that measured by the meteorological station (represented by the red point on the calibration graph) is:

$$V_{red}^{Ar} - V_{green}^{Ar} = (4.28 - 2.53) \pm 0.05mV = 1.75 \pm 0.05mV \quad (3.7)$$

This difference is not precisely the value at zero concentration V_{Ar}^{0-conc} , but as we already stated we expect an higher signal with Ar for the previously illustrated characteristics. Therefore if we translate all the linear regression by V_{Ar}^{0-conc} that we consider as the H_2O inside the gas, then we obtain a new estimation of the water concentration in the atmosphere that it is: $n_{H_2O}^{Ar} = (1.7 \pm 0.8)\%$ that it is now compatible with the meteorological measurements, even if with a less according compared to the calibration using air and with a very huge uncertainty. Therefore, it is possible that Argon actually provides a not-so-bad estimation of the water concentration in the atmosphere. Although the agreement with a perfect linear behaviour is not ideal (leading to high uncertainties), the results are not as poor as they might initially appear and is needed a deeper investigation of the composition of the inserted gas to establish with more accuracy if our hypothesis is correct.

3.2.3 Nitrogen

As we have done for the Ar case, we need to find the new resonance frequency, that we find experimentally as: $f_{N_2}^{res} = (839 \pm 2)Hz$. Then we do the measurements and report them in the following graph:

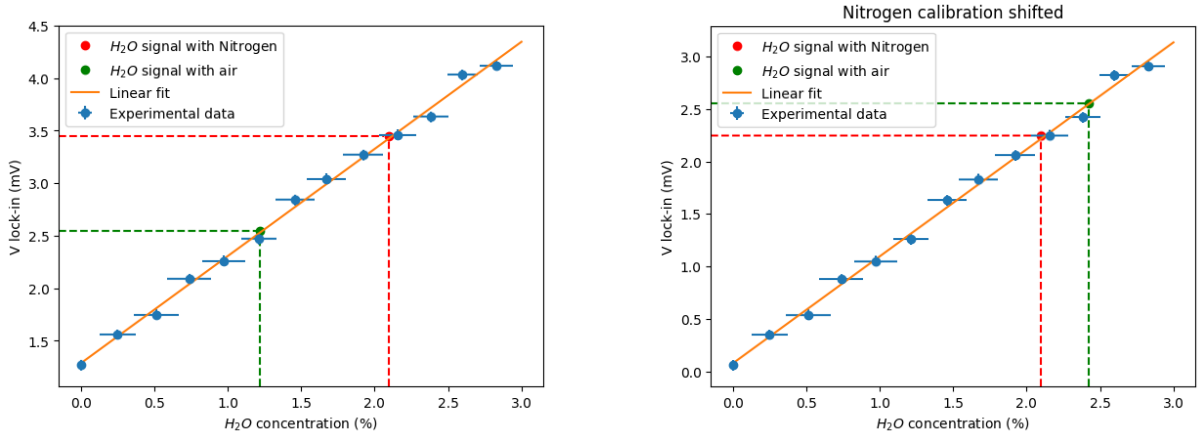


Figure 3.4: Calibration curve using N_2 : on the left the value with an offset due to residual humidity, on the right the same plot translated by $V_{N_2}^{0-conc} = (1.21 \pm 0.05)mV$

To obtain the concentration value of H_2O in the atmosphere, we follow the same procedure as with Ar . This involves extrapolating the concentration of H_2O from the lock-in amplifier voltage signal using linear regression. We then plot the green and red points, representing the lock-in voltage with only air inside the photoacoustic cell (which provides the water concentration) and the lock-in amplifier voltage needed to predict the correct H_2O concentration, respectively. For the afternoon of June 5th, this concentration is measured as $n_{H_2O}^{lab} = (2.1 \pm 0.1)\%$ (note a very stable measure during days as expected since meteorological conditions don't change a lot during

the experiment).

However, even in this case where we use a gas that is very similar to air, we obtain a water concentration value of $n_{H_2O}^{N_2} = (1.3 \pm 0.3)\%$, which, like with *Ar*, is incompatible with the real value obtained from the meteorological station. Instead, the angular coefficient, is: $m_{N_2} = (1.0 \pm 0.1) \frac{mV}{100}$ that it is, as for the Argon case, compatible with what we obtained with air within uncertainties. Noting the value of m_{N_2} we can state that also here we have a non-negligible difference in absorption properties that means a different interaction modality inside the photo-acoustic cell. In particular, in this instance we have more inhibition of the photo-acoustic effect with respect to the air, at the contrary of *Ar* in which we have a great enhancement of non-radiative relaxation processes. This can be caused principally by the difference in mass between the gases: N_2 is lighter than air, while *Ar* is heavier. The measurements with nitrogen (and also with *Ar*) will provide more useful insights in the second part of the experiment. The principal reason for switching to N_2 is to understand how the change in gas affects the results of our experiment. Using *Ar*, we anticipate results quite different from those obtained with air. However, with N_2 , being the most abundant component of air, we expect to obtain similar results. If there were differences, we aim to quantify the contribution of O_2 .

So, in the case of N_2 , we can see that the linear regression is a much better representation of the measurements compared to *Ar*, but it gives us a significantly different water concentration value. This result can be explained by considering that the propagation of sound waves is driven by the collective movement of atoms. Therefore, if there is a non-negligible difference in the gas in which the H_2O is introduced and relaxes in a non-radiative manner, this can lead to a markedly different effect on the physical process we are observing. We must not fall into the error of assuming that having "only" approximately 20% of the gas being different between pure N_2 and air means that only 20% of the measurement will change. Although the relationship between the lock-in value and the concentration of H_2O at low concentration is linear, the physical process on which the photo-acoustic effect is based is much more complex.

We note that also in this case we have a value of voltage different from 0 even if we let in only N_2 inside the cell. In this case that value is: $V_{N_2}^{0-conc} = (1.21 \pm 0.05)mV$, which is very similar to what we observed with *Ar*. This suggests that the effect is independent of the physical interaction between atoms and light, then it could be due to a small presence of water inside the gas, as previously supposed. However, in this case, the difference in voltages between "red" and "green" values is:

$$V_{red}^{N_2} - V_{green}^{N_2} = (3.47 - 2.53) \pm 0.05mV = (0.96 \pm 0.05)mV \quad (3.8)$$

This difference is less than the 0-concentration offset value, at the contrary of *Ar*. If we subtract this systematic error from all the values, we obtain a new H_2O concentration estimation: $n_{H_2O}^{N_2} = (2.4 \pm 0.3)\%$. This result is nearly compatible with the laboratory meteorological station measurement and represents a significant improvement compared to the initial estimation.

So we can conclude that from the analysis of the angular coefficient the interaction inside the cell are very different between N_2 and *Ar* compared to the air, with a much higher distance from a linearity behaviour and absorption properties in the *Ar* case. It is not so surprising because *Ar* and air are very different gases even

if, as we have seen from the N_2 case, a not predominant difference in the background gas does not mean a negligible difference in the estimation of water concentration inside the atmosphere because of the complexity of the photo-acoustic effect. Then the best gas for the estimation of water concentration inside the atmosphere is air, although N_2 is also a good choice but with a light overestimation; while Ar even if very different between air, gives reasonable mean value with the very problematic higher uncertainty related to the non-linearity trend of the data.

To give a faster and simpler reading of what we have just shown, we report below a summary table of the H_2O concentration (Table 3.1) and angular coefficient of the linear fit (Table 3.2).

	First Measure (%)	Eventual Correction (%)	$n_{H_2O}^{lab}$ (%)
$n_{H_2O}^{wider}$	(1.9 ± 0.5)	/	(1.8 ± 0.1)
$n_{H_2O}^{narrower}$	(2.0 ± 0.6)	/	(1.9 ± 0.1)
$n_{H_2O}^{Ar}$	(0.9 ± 0.8)	(1.7 ± 0.8)	(2.0 ± 0.1)
$n_{H_2O}^{N_2}$	(1.3 ± 0.3)	(2.4 ± 0.3)	(2.1 ± 0.1)

Table 3.1: Table of different water concentration in different conditions

	Air (narrower) $\left(\frac{mV}{100}\right)$	Ar $\left(\frac{mV}{100}\right)$	N_2 $\left(\frac{mV}{100}\right)$
$m_{linear fit}$	(1.2 ± 0.2)	(1.6 ± 0.4)	(1.0 ± 0.1)

Table 3.2: Table of different angular coefficient of linear fit for water calibration

Now we go towards the second part of the experiment, in which we try to study the behaviour of the signal during time to understand better what really happens inside the photo-acoustic cell.

3.3 Stability analysis

In order to understand the physics inside the cell a stability analysis of the signal is performed for the case of injected gases: Air and Nitrogen in a deep way, while Ar is analyzed only from a very qualitative point of view. Ar is analyzed to understand better the change in the experiment changing radically the gas inside the photo-acoustic cell. On the contrary N_2 is properly used because slightly different compared to the air. Measurements of the lock-in signal and pressure inside the cell are taken as a function of time: every 15s these data are taken for 15 minutes (900s). Two different water pressures are chosen: $P_{H_2O}^{high} = (22.0 \pm 0.5)mbar$ for the high one and $P_{H_2O}^{low} = (6.0 \pm 0.5)mbar$ for the low one, as we want to see the variation of the signal for a high water concentration and for a low one. The speed at which the gas is inserted is also varied (for the second and third section) and in the following plots we refer to: "fast" as reaching $(840 \pm 1)mbar$ (the total pressure inside the cell) in about 30 seconds, while *slow* refers to about 15-20 minutes letting into the cell 2mbar of the gas per time.

3.3.1 Condensation and Losses

As previously stated in Chapter 2 of this paper, the primary objective of this part of the experiment is to determine the time required to achieve a stable signal, considering the potential impacts of condensation and losses on the voltage readings from the lock-in amplifier. We conduct the experiment under the most challenging conditions: maximum partial pressure of H_2O and the fastest possible air injection into the photoacoustic cell. Although the effect of varying gas injection speeds will be examined in subsequent studies, we proceed by measuring the lock-in signal variation over 800 seconds (registering a value every 30s) at a partial water pressure of $P_{H_2O} = 28.0 \pm 0.5 \text{ mbar}$. The photoacoustic cell is sealed at a pressure of $P = (840.6 \pm 0.2) \text{ mbar}$ (as for all measurements in this experiment we stayed in the range of pressure $P = (840 \pm 1) \text{ mbar}$). The corresponding voltage and pressure data over time are presented in the figures below:

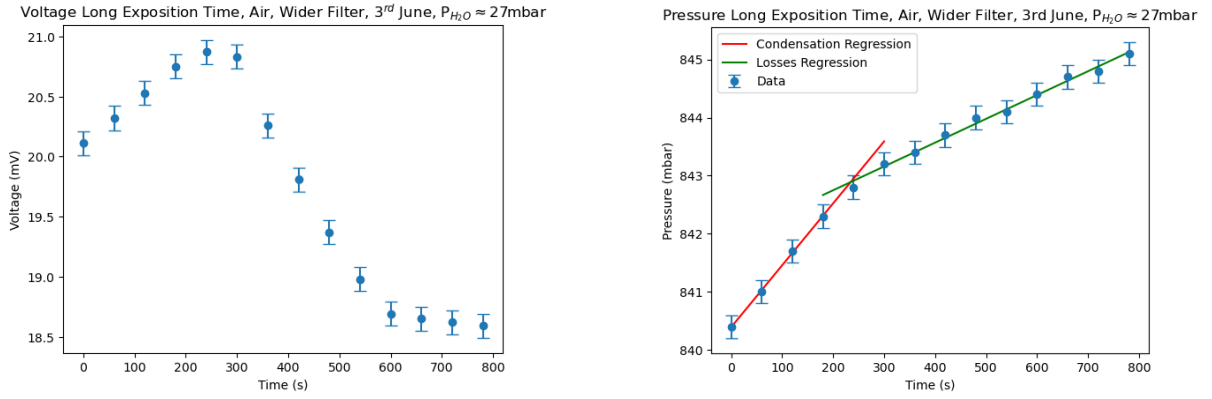


Figure 3.5: Pressure and Voltage during the initial measurement to determine the stabilization time

Figure 3.5(a) displays a pattern that, recurs throughout this study: an initial increase in the signal, peaking around $t \approx 230$ seconds, followed by a rapid decline to a stable value within the 600-700 second interval. This suggests that a waiting period of approximately 11 minutes is optimal for signal stabilization. The initial voltage increase until the maximum is attributed to the re-evaporation of water vapour condensed on the cell walls due to the rapid air compression. The subsequent rapid decrease is likely due to the non-radiative relaxation processes leading to energy dissipation via inelastic collisions, eventually reaching a stable gas condition with minimal further decay. The maximum is the trade-off point between the water evaporation (the signal increase) and the energy loss via collisions (the signal decrease) that are always present.

This hypothesis is corroborated by Figure 3.5(b), which shows the pressure behaviour over time. Initially, for the first ≈ 250 seconds the pressure increases rapidly at a rate of $(P/t)_{\text{condensation}} = (0.011 \pm 0.002) \text{ mbar/s}$, corresponding to the voltage increase. This is followed by a slower pressure increase rate of $(P/t)_{\text{losses}} = (0.0041 \pm 0.009) \text{ mbar/s}$, approximately one-third of the initial rate, indicating losses and potential H_2O desorption from the cell walls.

To verify our assumptions, we also measure pressure variations inside the photoacoustic cell in the absence of H_2O under pressures of $P = (840.2 \pm 0.2) \text{ mbar}$ and $P = (0.9 \pm 0.2) \text{ mbar}$. These measurements provide insight into the errors when attempting to maintain very low water pressures within the cell. The results are illustrated

in the following figures:

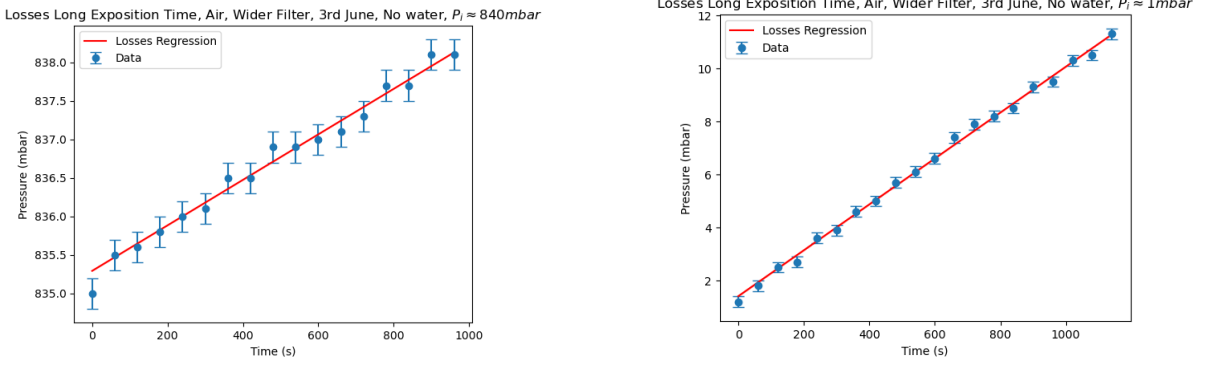


Figure 3.6: Pressure over time with no H_2O present at $P = (840.2 \pm 0.2) \text{ mbar}$ (left) and $P = (0.9 \pm 0.2) \text{ mbar}$ (right)

In the pressure graph 3.6(a), the initial data points are excluded from the linear regression due to their rapid acquisition during a transient state, rendering them outliers. As anticipated, losses are more significant at lower pressures compared to near atmospheric one, attributed to the greater pressure difference between the photoacoustic cell and the environment. We obtained a pressure increase rates of $(P/t)_{\text{losses}}^{840 \text{ mbar}} = (0.0029 \pm 0.0004) \text{ mbar/s}$ and $(P/t)_{\text{losses}}^{1 \text{ mbar}} = (0.0086 \pm 0.0008) \text{ mbar/s}$ for the left and right graphs in Figure 3.6, respectively. The rate at high pressure without added water is comparable to the $P_{H_2O} = (28.0 \pm 0.5) \text{ mbar}$ case, albeit lower, suggesting minor H_2O de-adsorption from the cell walls, contributing to measurement error due to pressure value oscillations.

The pronounced pressure increase rate at low pressures indicates an inherent and significant error in concentration measurements, that we estimate in this way: both to have a high value of water pressure and to have a low value of P_{H_2O} inside the cell, we estimate that on average we needed $t \approx 60 \text{ s}$ from isolating the cell from the membrane pump to filling the cell with water at the desired pressure. This happens because at every pressure (high or low) we need to be very accurate and then we need approximately the same time to obtain the desired initial water pressure inside the cell. This causes a flat error as: $\sigma_{P_{H_2O}} = 0.5 \text{ mbar}$.

Henceforth having said that, pressure values will not be presented in subsequent experiments because all the pressure variation during time will be almost equal between themselves. The focus will shift to confirming the hypotheses regarding condensation and energy loss due to inelastic collisions, rather than calibration improvements for stable signal acquisition.

3.3.2 Argon

We begin our investigation with Argon (Ar) due to its significant differences from the air (unlike N_2 , which constitutes approximately 80% of air) in order to assess how completely changing the "background gas" might affect the interaction dynamics. Our goal is to determine whether the same qualitative behaviour observed previously, can be detected. Thus, the primary aim of using Ar as the background gas is to provide insights into a potentially more general interaction process, even though our examination of Ar remains at a preliminary

stage without delving into detailed theoretical treatment.

The following figures present the voltage values obtained from the lock-in amplifier at H_2O pressures of $P_{H_2O} = (22.2 \pm 0.0.5)$ mbar and $P_{H_2O} = (5.9 \pm 0.5)$ mbar:

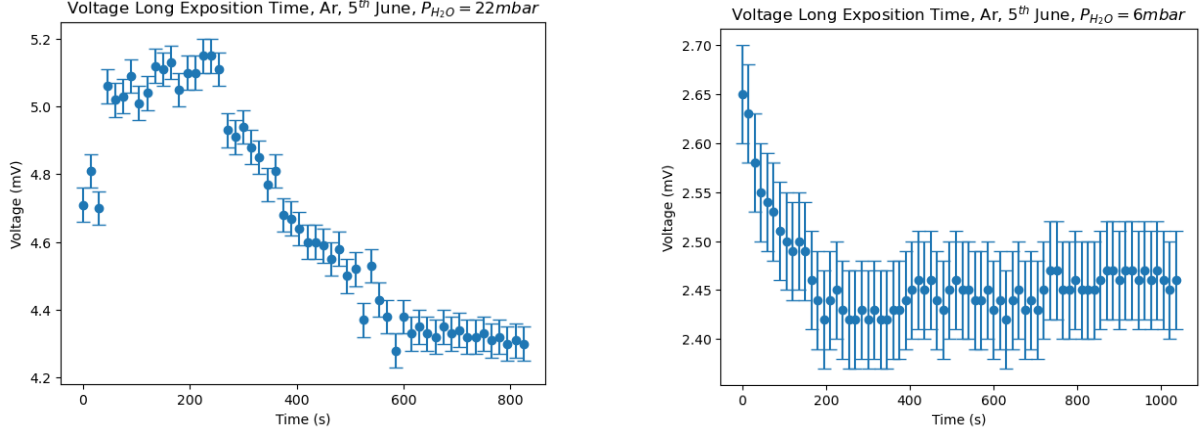


Figure 3.7: Voltage behavior obtained from the lock-in amplifier with *Ar* at $P_{H_2O} = (22.2 \pm 0.5)\text{mbar}$ (left) and $P_{H_2O} = (5.9 \pm 0.5)$ mbar (right)

We note that for these type of graph in which we take measurements every 15s, the plot with the errorbar is very confusing, then for all the other measurements the errorbar is omitted. The two voltage behaviours shown in the figures are markedly different. At low H_2O concentrations, as expected, there is no visible condensation (corroborated by both the graph and direct observation), resulting in the absence of the initial voltage increase and only a rapid decrease. Notably, the low concentration graph (Figure 3.7(b)) displays a surprising feature: after the initial decrease, there is no minimal decay as observed in the air case, but at the contrary a slow increase in voltage value (approximately 0.05 mV over 800 seconds). This phenomenon will be further investigated in the context of air and N_2 .

Our primary interest lies in determining whether the photoacoustic effect significantly changes when using *Ar* instead of air. Initial data analysis suggests that substituting air with *Ar* does not result in drastic differences: there is an initial increase due to condensation, followed by a rapid decrease, and then a stable value with minimal further decrease (focusing on the high H_2O concentration for the moment, as there is no comparable low concentration data with air yet). Some differences do exist, such as a more rapid initial voltage increase, a temporary stabilization phase, and a less rapid decrease compared to the air case, reaching a stable phase approximately 50 seconds later. This supports the calibration findings indicating that *Ar* has poorer thermal conductivity, facilitating higher pressure wave values (peaks) and slower energy dissipation (manifested as a less rapid post-peak decrease). Nonetheless, *Ar* should not be excluded as a comparable background gas to air in the photoacoustic interaction with H_2O .

3.3.3 Nitrogen

In the case of Nitrogen (N_2), the pressure of the injected gas is varied to assess whether condensation is enhanced and to determine if the gas inside the cell responds to the energy differences of the "background gas". We use $P_{N_2}^{low} = (2.0 \pm 0.2)bar$ for the "low-pressure" scenario and $P_{N_2}^{high} = (6.0 \pm 0.2)bar$ for the high-pressure scenario. The variation in the gas injection method aims to understand if condensation can be mitigated through a more "reversible" approach.

For clarity and ease of result interpretation, we discuss the two different H_2O concentration cases in separate sections. This structure facilitates the orderly presentation of results and underscores that the comparison between the two H_2O concentrations is not of fundamental interest.

6mbar

We start our discussion for the case of $P_{H_2O} = (6.1 \pm 0.5)mbar$ of water pressure inside the cell.

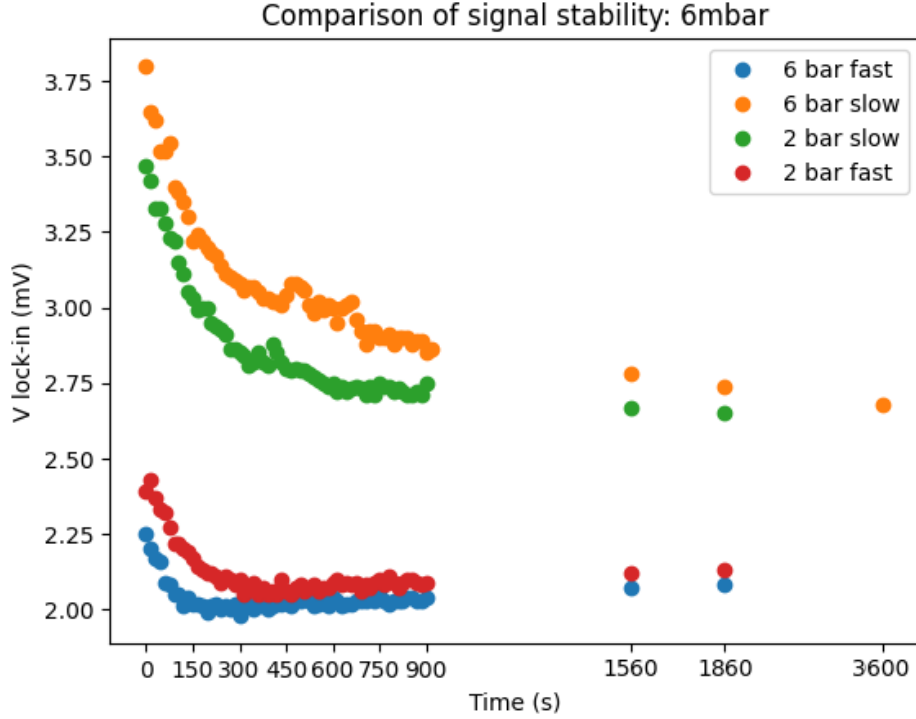


Figure 3.8: Comparison of different inserting gas procedures and injected gas pressures, the x-axis scale is varied between 1860s and 3600s

From the plot, it can be observed that all signals initially decrease, indicating that condensation is not present due to low concentration of water, as previously noted with Ar . The signal decrease is notably longer and smoother for the *slow* methods compared to the *fast* ones. The initial dip in the signal is likely due to energy dissipation resulting from molecular collisions with the chamber walls. When the gas is introduced slowly, the energy dissipation is less due to entropic reasons compared to faster methods, as illustrated in Figure 3.8. It is hypothesized that with sufficient time, thermalization with the environment will equalize the signals, resulting

in a rise for the *slow* methods and a continuous decrease for the *fast* methods.

We also note that the voltage signals for the same method of introduction (*fast* with *fast* and *slow* with *slow*) but at different pressures, are more similar compared to signals for different methods at the same pressure. This suggests that higher kinetic energy has a lesser impact on the non-radiative relaxation of H_2O molecules compared to the method of gas introduction at least in the case of low water concentration; which aims for a more "reversible" transformation of H_2O .

Consequently, the difference between the same method of N_2 introduction but at different pressures is more pronounced at higher pressures. The *slow* method enhances the photoacoustic process, which is further amplified by the higher kinetic energy of N_2 molecules. Conversely, the *fast* method results in a significant temperature decrease inside the gas (the increase in the *fast* methods is due to thermalization of N_2 with the laboratory environment). This effect is intensified by the higher kinetic energy of the gas at higher pressure, leading to a greater temperature decrease and consequently a very low signal measured by the lock-in amplifier.

22mbar

We expect a qualitatively different behaviour when switching between the *fast* and *slow* methods of gas introduction. Specifically, we anticipate minimal or no condensation in the *slow* method, contrary to the *fast* method. The comparative plot is provided below:

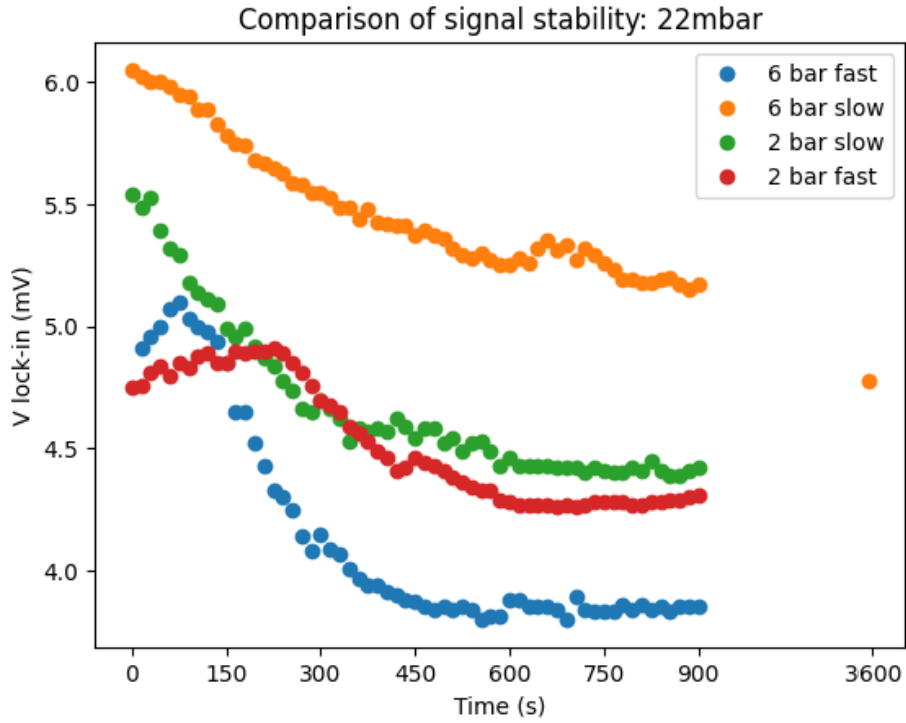


Figure 3.9: Comparison of different gas injection procedures and pressures at $P_{H_2O} = (22.1 \pm 0.5) \text{ mbar}$, the x-axis scale is varied between 900s and 3600s

For the case of $P_{H_2O} = (22.1 \pm 0.5) \text{ mbar}$ water pressure, an initial rise in the signal is observed for the *fast* methods, as expected. This increase is likely due to the evaporation of water vapour that condenses when the

gas is introduced rapidly. This rise is not observed in the *slow* signals, as the gentle introduction of gas prevents water vapour condensation. The subsequent decrease in all signals is attributed to energy dissipation, as seen in the 6 mbar cases. Notably, the *fast* values are lower than the *slow* values, likely due to entropic reasons. If we wait long enough, thermalization is expected to equalize the signals because higher tension values tend to decrease due to slow energy dispersion to the environment. In contrast, *fast* signals gain energy from the environment due to initial energy loss when N_2 is introduced.

Interestingly, the "order" observed in the 6 mbar cases is preserved here (i.e., $V_{6bar}^{slow} > V_{2bar}^{slow} > V_{2bar}^{fast} > V_{6bar}^{fast}$), but the two "2 bar" signals are very similar after the decrease, whereas the two "6 bar" signals differ by approximately 35%. This differs from the 6 mbar cases, where the *fast* and *slow* signals were similar. This discrepancy likely arises because, in the 6 mbar cases, a large amount of N_2 interacts more homogeneously with H_2O , while in the 22 mbar cases, H_2O molecules interact more with each other than with N_2 , leading to different results.

In this case, the lock-in voltage values stabilize over a longer time compared to the 6 mbar cases. Specifically, for V_{6bar}^{slow} , the voltage change between $t = (500 \pm 1)$ s and $t = (900 \pm 1)$ s is (0.27 ± 0.05) mV, double the change observed in the previous case. This is due to more heat being released from the non-radiative relaxation of H_2O , requiring more time to thermalize with the environment at higher temperatures. Consequently, V_{2bar}^{fast} is more similar to V_{2bar}^{slow} than in the 6 mbar case and has a lower increase due to more H_2O molecules generating heat and losing energy non-entropically. Additionally, condensation allows N_2 molecules more time to lose energy to the photoacoustic cell walls rather than to H_2O molecules, leading to a higher temperature compared to the previous case.

Lastly, the time to re-gasify condensed H_2O differs significantly between the *fast* methods at different N_2 pressures. The higher pressure gas takes approximately half the time to complete the re-gasification of H_2O from liquid to gas compared to the lower pressure gas: $t_{peak}^{blue} = (125 \pm 1)$ s, $t_{peak}^{red} = (265 \pm 1)$ s, where "blue" and "red" refer to the colours in Figure 3.9. This is likely because N_2 at $P_{N_2} = (6.0 \pm 0.2)$ bar interacts more energetically with the condensed H_2O , forcing re-gasification and negating the previously described time-gaining effect.

3.3.4 Air

For the case of Air, the injected gas pressure is not varied, it is always the atmospheric pressure: $P_{air} = (982 \pm 2)$ mbar because we use directly the air inside the laboratory, without any construction of apparatus that can modify its pressure. As for the case of N_2 we start the discussion for the case in which we used $P_{H_2O} = (6.1 \pm 0.5)$ mbar and after we switch to the case of higher water partial pressure $P_{H_2O} = (22.1 \pm 0.5)$ mbar.

6mbar

The graph of the variation of the voltage signal in the lock-in for the case of $P_{H_2O} = (6.1 \pm 0.5)$ mbar is reported below:

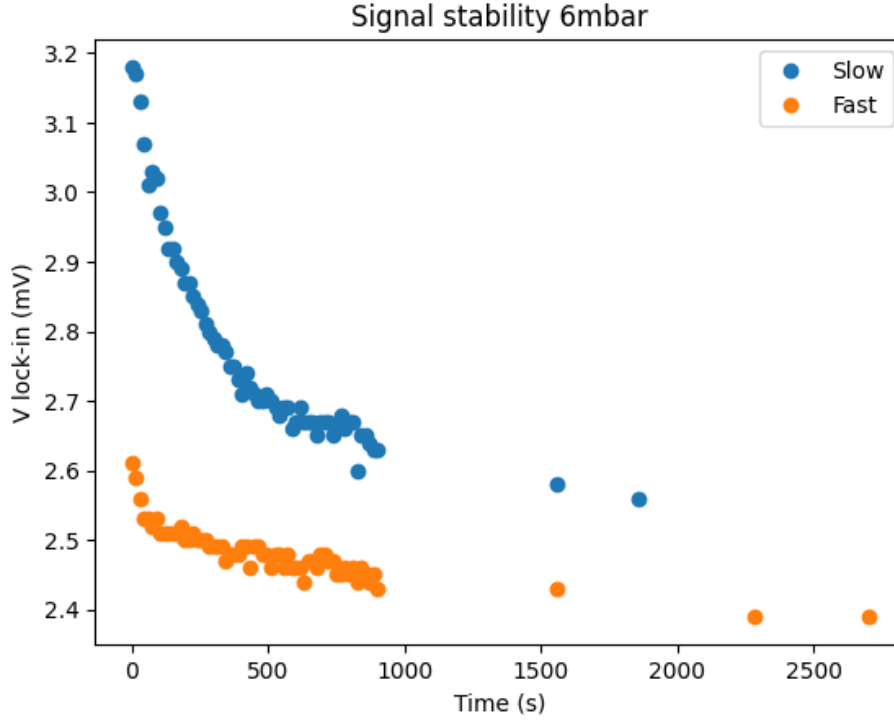


Figure 3.10: Comparison of different inserting gas procedures

We can see from the plot that the *fast* way signal is bigger than the *slow* one which is consistent with what it is mentioned before. We also note that in *fast* we have no tendency of low increasing that is present at the contrary in both Ar and N_2 . This is explainable from the fact that air is let in with a pressure that is $\frac{1}{2}$ compared to the pressure with which we do the measurements in the case of air compared to the other two gases (with which we did the calibration at $P_{Ar/N_2} = (2 \pm 0.2)bar$). This difference in the pressure can cause less cooling of the gas inside the cell that needs to thermalize less with the environment and reach the equilibrium phase in less time.

Moreover is evident that in this case the difference between the *fast* and the *slow* is not so pronounced as in the case of N_2 in 3.8. With air we have a difference in voltage between the 2 ways of proceeding at $t = (800 \pm 1)s$ that is $\Delta V_{air}^{800s} = (0.23 \pm 0.05)mV$, while in the case of N_2 is: $\Delta V_{N_2}^{800s} = (0.58 \pm 0.05)mV$. This huge difference is related, again, to the difference in pressure between the two cases, which gives a much higher time to have the real stable value when the gas will completely thermalize with the environment.

Is important to note that this huge difference in ΔV is more related to the very low signal in the *fast* for the case of N_2 (for both pressures since they are similar both in *fast* and *slow*); indeed the two *slow* curves are very similar, this is again an evidence that the main difference between N_2 and air is not related to the gas in itself that we use, but mainly, at least at low H_2O pressure, to the pressure at which we do the measurements. "Pressure effect" that, as we have already seen from the comparison 3.8, is downed by the way in which we let in the background gas.

This is a piece of evidence that confirms that N_2 is probably a good choice for the calibration but with at a pressure that is more similar to the atmospheric one, or using much more time to let in N_2 inside the photo-

acoustic cell (improvements that are the same for Ar).

22mbar

We report finally the plot for the comparison of *fast* and *slow* for the air, but in the case of high H_2O concentration:

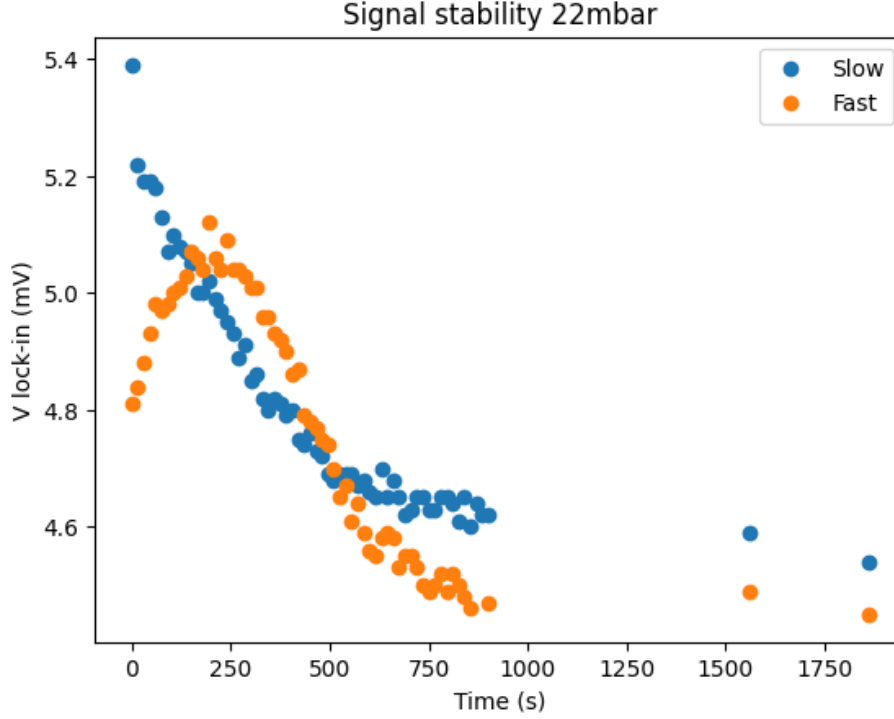


Figure 3.11: Comparison of different inserting gas procedures with air

Firstly we note that the *fast* is very similar to what we have already seen in 3.5 (in a qualitative way, taking into account the trend of measurements, not the single value since are used 2 different filters), this means that our measurements are repeatable to a few days' difference that was expected not only as for the fact that repeatable of an experiment has to be one of its main pillars, but confirms also the fact that from the 3rd June to the 7th June, the atmospheric conditions were substantially always the same.

One important thing to note is that in this case the results obtained by this graph, are qualitatively similar to what we have obtained in the case of N_2 in 3.9 for the "2 bar" case (also here, only "qualitatively" because we have the same difference in voltage signal that what we highlighted in the calibration part). This is perfectly in agreement with what we said when we analyzed N_2 : at high value of water concentration is much important the difference in pressure than the way in which we work. In that case we said it to compare very different gas injected pressure: $(6.0 \pm 0.2)bar$ and $(2 \pm 0.2)bar$. In this case, we want to compare air at atmospheric pressure (so around $1bar$), to the condition in which we did the calibration with N_2 that is at $(2.0 \pm 0.2)bar$ so we take into account only the "red" and "green" line of plot 3.9. The difference in pressure is a lot because we doubled the pressure, but not so high as in the comparison between different pressures in N_2 . Then we see a quite

perfect agreement in the trend of the signal between N_2 case and air: an intersection between the two curves around $t \approx 200s$, a peak around $t \approx 250s$, a decrease and a stabilization around $t \approx 700s$. This consideration means that the physical effect inside the photo-acoustic cell is not much different in N_2 compared to air, and then "promote" N_2 as a good choice to do the calibration, even though air is better in any case as we have already seen in the calibration part of the data analysis. This comparison confirms our hypothesis on the fact that the N_2 (and then maybe also Ar since the intercept in the calibration curve is very similar) is probably not completely dry.

As expected the condensation in *slow* is not present, at the contrary of *fast* as we highlighted yet.

So having a very similar qualitative behaviour, we expect that N_2 could be a good choice for the calibration part, although it is necessary to conduct a deeper investigation to be sure that our assumption of "non-dry" gas is correct.

Chapter 4

Conclusion

In all the experiment we reach to demonstrate the possibility to measure the water concentration in the atmosphere using the photo-acoustic effect. Firstly changing the filter from a wider to a narrower one, and after instead of using air we change the background gas using N_2 and Ar : the first one to obtain evidence of what changes if we change only in a non-majority part of the gas that interacts with H_2O , the latter to have an idea of the change in the interaction behaviour if we change completely the gas inside the cell that interact with water. All the three cases give compatible results between the air one and the data from the meteorological station inside the laboratory. However, this agreement is possible only assuming that the signal at 0-concentration of H_2O inside the cell is given by a systematic error that causes a rigid translation of the graph due to the presence of H_2O inside N_2 and Ar , that present offset very similar. Moreover is interesting to note from the angular coefficient of the linear regression that N_2 disfavors the non-radiative relaxation process of H_2O compared to air, instead Ar enhanced this way of relaxation. Then we obtain a slight overestimation with N_2 and a slight underestimation with Ar . Is important to note that for Ar the linear fit seems a bit "forced" which translates to very huge uncertainties.

On the other hand, during the second part of the experiment, we try to understand better the physical processes that happen inside the photo-acoustic cell focusing on the variation in time of the values of tension principally of N_2 and air at high and low water concentration, and changing also the way with which we let in the gas inside the photo-acoustic cell: very slow or fast. At the start of the experiment, these measurements of tension over a long-time gives us the possibility of quantifying the losses and the condensation inside the cell, noting that losses are non-negligible, especially at low pressure. It confirms moreover that at the time in which we see a maximum in voltage, we have a change in the slope of increasing rate of pressure, due to the fact that condensation stops being present and there is only losses-process. We have a maximum in the tension because at that point we have the trade-off between condensation and collisional relaxation processes, with the latter becoming the predominant and then we see a rapid decrease in signal.

After that, we concentrate more on the proper investigation of the interaction inside the photo-acoustic cell changing the "boundary conditions" as just stated, with the addition that in the case of N_2 we vary also the pressure. We observe the same qualitative behaviour principally between N_2 and air, but also for Ar that is not

deeply studied. So is observed: at high water concentration and with the fast way of letting in the gas we see an initial increasing of tension due to condensation and then a rapid decreasing due to inelastic collision between atoms. Then for the low water concentration, where we don't see the condensation part, we observe only a decreasing (more or less rapid, if we focus on "*fast*" or "*slow*" modality) and after 11 minutes (the estimated time to have a stable value) we identify a slight tendency of increasing (more in N_2 rather than in air) due to thermalization. The thermalization gives instead a slight tendency to decrease in voltage at low pressure of the background gas and high water concentration.

With a slow way to introduce the gas inside the cell, we have no condensation (also at $P_{N_2} = (6.0 \pm 0.2)bar$), a less loss of energy because of the less entropic contribution and a slow continue of decreasing. Higher pressure gives me a higher signal if "*slow*", again for entropic causes. The higher pressure and the slightly different interaction process inside the cell for N_2 return the idea that the air background gas is the best in terms of efficiency in time and the absolute value of concentration estimation. N_2 represents quite the same qualitative behaviour of air, but is always present, as in the calibration part, a discrepancy in terms of absolute value of tension compared to air that confirms what is highlighted in the calibration part explained as "non-dry" gas, even though there is no thorough study of the gas composition within the background gas. While the very low qualitative different behaviour is mainly referred to the non-negligible presence of O_2 inside air evidently not present in N_2 (as expected).